Using meteorologically based dynamic model to assess malaria transmission dynamic among under five children in an endemic region

Yazoumé Yé [1§], Catherine Kyobutungi[1], Moshe Hoshen[2],

[1] African Population and Health Research Centre, PO Box 10787, 00100 GPO Nairobi, Kenya, + 254 020 2720 400, Fax + 254 020 2720380
[2] Braun Hebrew University-Hadassah School of Public Health and Community Medicine, P.O. Box 12272 Jerusalem 91120. Israel

§Corresponding author
Emails:
YY: yyazoume@aphrc.org
CK: ckyobutungi@aphrc.org
MH: mosheh@ekmd.huji.ac.il

Abstract

Background

To support malaria control strategies, prior knowledge of disease risk is necessary. Developing a model to explain the transmission of malaria, in endemic and epidemic regions, is of high priority in developing health system interventions. We develop, fit and validate a non-spatial dynamic model driven by meteorological conditions that can capture seasonal malaria transmission dynamics at a village scale in a malaria holoendemic area of north-western Burkina Faso.

Methods

676 children aged 6-59 months took part in the the study. Trained-Interviewers visited at home weekly from December 2003 to November 2004 for *Plasmodium falciparum* (*P falciparum*) malaria infection detection. Anopheles daily biting rate, mortality rate and growth rate were evaluated. Digital meteorological stations measured ambient temperature, humidity and rainfall in each site.

Results

The overall *P falciparum* malaria infection incidence was 1.1 episodes per person year. There was a strong seasonal variation of the *P falciparum* malaria infection incidence with a peak observed in August and September corresponding to the rainy season and with a high number of mosquitoes. The model estimate of monthly mosquito abundance and the incidence of malaria infection correlate well with observed values. The fit was sensitive to daily mosquito survival and daily human parasite clearance.

Conclusion

The model has shown a potential for local scale seasonal prediction of *P falciparum* malaria infection. It could therefore be used to understand malaria transmission dynamics using meteorological parameters as the driving force and to help district health in identifying the risk period for more focused interventions.

Keywords: Meteorology, local scale, modelling, prediction, *Plasmodium falciparum* malaria, underfive year, endemic region

Introduction

Malaria continues to be a deadly disease, and action towards its control remains challenging for researchers and policymakers. To support control strategies, prior knowledge of disease risk is necessary. Developing a model to explain the transmission of malaria, in endemic and epidemic regions, is of high priority in developing health system interventions. As malaria is a vector-borne disease, and the life cycle of its vector drives the transmission, the female Anopheles mosquito. This life cycle, as well as that of the within-vector parasite, in turn is dependent on the microclimate.

Since the early 20th century, there have been attempts to understand malaria transmission dynamics, through mathematical modelling, to support control efforts. Ross developed the first model to predict malaria transmission and spread of the disease, and later concluded that increasing vector mortality significantly could eradicate malaria [1, 2]. In the 1950s, George Macdonald, building on Ross' model, concluded that, at equilibrium, the weakest link in the cycle of malaria transmission is the adult female *Anopheles* [3]. His conclusions formed the basis of the global malaria eradication campaign, with DDT targeted at adult female *Anopheles.* In the 1970s, Dietz and Molineaux, in the Garki project, developed a more sophisticated model, clearly considering human immunity interacting with transmission [4, 5]. The model was correct in its ability to simulate malaria epidemiology in Garki, given entomological input, and it provided comparative forecasts for several specific interventions [6].

Further, Halloran and colleagues clearly considered the population-level effects of potential stage-specific vaccines [7]. Since then, malaria modelling has drawn significant attention. The development of computers has allowed the basic concepts of various compartmental models to be reduced to the individual level. Populations are modelled as large numbers of interacting individual humans and individual mosquitoes, each with its own characteristics and dynamics [6]. Further steps toward biological realism have begun to include the effects of weather [8, 9, 10, 11, 12, 13, 14, 15, 16].

The lack of data in many components of malaria transmission has restricted modelling efforts to a regional scale, since a significant pool of data is needed to test and fit the different sets of parameters. Even though available models are informative for developing global, regional or national malaria control strategies, they are limited in their applicability at local sites. However, local conditions are the main drivers of malaria transmission [17]. Thus, better understanding of these conditions and transmission dynamics through modelling may be more informative and relevant for local control efforts.

This study elected to develop and validate a non-spatial dynamic model, driven by meteorological conditions, which can capture seasonal malaria transmission dynamics, at the scale of a single village. This was achieved by using comprehensive field data that include incident cases of human *P falciparum* malaria infection, as well as entomological and meteorological data. The focus for human infection was on children under five years,

since they are the most vulnerable, and because most infections in this age group will be symptomatic and, therefore, more easily detected.

Methods

Study sites

The study was conducted in the town of Nouna and the villages of Cissé and Goni. These three sites are part of the *Nouna Demographic Surveillance Systems* (DSS) area [**Error! Reference source not found.**]. Others detail description are given elsewhere [19].

Study population

676 children (Cissé: 171, Goni: 240 and Nouna: 265), aged 6 to 59 months, took part in the study. The children were selected at each site by systematic cluster sampling of households from the DSS database. Description of the study population is given elsewhere [20**].**

Active case detection: P falciparum infection

In each site, site-based interviewers visited weekly the children to assess their *P falciparum* malaria infection plasmodium status and collect housing conditions data. The case detection methods are extensively described in Yé and Colleagues [20]. The outcome measure was a *Pf* infection episode, defined as an axillary temperature >= 37.5°C plus a positive parasite test.

Entomological data

Mosquito population abundance was monitored using a standard CDC Light Trap (LT) [21] from December 2003 through November 2004. Mosquitoes were captured on the 1st and 2nd day of each month at each site in four randomly selected houses.

LT fitted with incandescent bulbs were installed close to human volunteers sleeping under untreated mosquito nets in these houses for two consecutive nights from 18:00 to 06:00 hours. In addition, we used the Human Landing Collection (HLC) method, which involves one person sitting inside an uninhabited house and another outside, collecting mosquitoes that land on their exposed legs using torchlight and test tubes. This was done in two shifts (18.00 to 24.00 hours and 24.00 to 06.00). HLC volunteers gave informed consent. They were given malaria prophylaxis and checked for fever for a fortnight after their participation in the study.

Field supervisor transported the mosquitoes caught to the laboratory in a cold-box. A technician in entomology counted and sorted by species the specimens. He classified mosquitoes caught by LT and HLC as ‘unfed’, ‘partly-fed’, ‘fully fed’, ‘semi-gravid’ or ‘gravid by external inspection (LT) or dissection (HLC). The technician checked for

parity the ovaries of unfed HLC mosquitoes as described by Detinova [22] and Gilles & Warrell [23].

The age structure of the *An. gambiae* population was assessed by calculating the parity (number of times eggs laid previously). A high fraction of *nulliparous mosquitoes (*mosquitoes that had never laid eggs) means a young population. This help to estimate the proportion of infectious vector to calculate the value of infectious bite rate parameter.

Indoor human bite rates [3] were calculated for each month and site, as follows: Human bite rate: $ma = Bs/P\ \ /n$, where *Bs* is the number of *An. gambiae* caught indoor by HLT; *P* is the number of people involved in the capture, and *n* is the total number of nights.

An. gambiae mortality (*k-value*) was calculated of each month and site. This expresses the number of vectors surviving from the egg stage to the adult stage. The monthly number of vectors was transformed into a natural logarithm. For a month with none vectors the logarithm of one was calculated. Based on previous studies, we assumed the maximum number of eggs oviposited by individual mosquitoes was, *m*=100 eggs [24, 25] on average. To calculate *k-value* the following formula was: log(potential eggs, month 1) = log (adults+1, month 1) + log(maximum individual fertility), and K_{month1} = log (potential eggs, month 1) - log(adults+1, month 2). [26]. The resulting *k-value* was used to calculate the monthly mortality rate (*m*), important parameter of our model, using the formula: $M = 1 - 10^{-kvalue}$.

Measurement of meteorological parameters

Sites based meteorological units measured rainfall, temperature and humidity on the ground. Unit were set for 10-second measurement cycles and 10-minute recording cycles. Detail is given elsewhere [20]

Model development

Model description

The model was based on the so-called compartmental model developed by Ross [1] and adapted by MacDonald [3]. These models were based on the assumption that the human population can be subdivided into three compartments: 1) *Susceptible*: do not have malaria; 2) *Infected*: have the parasite, but it has not yet developed to the gametocyte stage; and 3)_*Infectious*: are symptomatic and have the parasite at the gametocyte stage. Similarly, the vector population can be classified as: 1) *Susceptible* (do not carry the parasite); 2) *Infected* (fertilization and sporogony); and 3) *Infectious* (sporozoites in the salivary glands). The transmission process started when an infected vector takes a blood meal from a human. The changes among the subpopulations in each compartment are determined by a set of parameters, like mosquito mortality, bite rate, growth rate, sporogony and gonotrophic cycle duration, and human malaria-induced mortality and parasite clearance rates. Most malaria models were constructed on these basic assumptions, and so was the Mckenzie and others [27] model from which our model is

derived. In our model, the mosquito population was divided into two subpopulations, non-infected and infected, since we assumed that every mosquito that feeds on an infected human would have about 100% probability of becoming infectious if it survived long enough. The state and transition of the model (Figure 1) shows the changes in each subpopulation given different parameters. These parameters are labelled with Greek characters and defined in Table 1. This model is an extension of previous model which was set to detect malaria in the dry season [28]. This model was driven by entomological data and did not simulate le dynamic of the vector population. The current one has vector population dynamic which is driven by temperature and rainfall. Since the dry season in the study region is characterised by total absence of rainfall a model driven by rainfall may not be appropriate to capture transmission. The appendix provides the details of the mathematic expressions of the model and the specific assumptions.

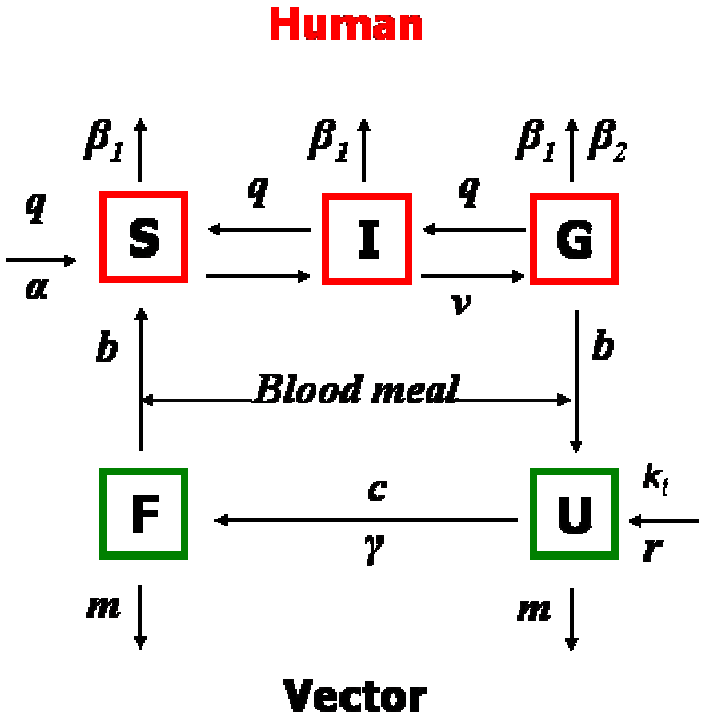

Figure 1: State and transition of the dynamic model. Human: S: susceptible, I: infected, G: infectious; Vector: U: susceptible, F: infectious

Table 1: Definition of model parameters

Parameters	Definition	Source
α	Daily natural per-capita human birth rate	DSS_ Recalculated in daily birth rate
β_1	Daily natural per-capita human death rate	DSS_ Recalculated in daily death rate
β_2	Daily malaria-induced per capita death rate in humans	Noun DSS_ Recalculated in daily death rate

q	Daily malaria clearance rate in humans	Fitted and compared with field data
v	Time delay for human host, from becoming infected to becoming infectious	Dietz *and others*. 1974 ; Gu *et al*. 2003
m	Daily mortality rate of vectors	Calculated and fited
r	Daily mosquito per-capita intrinsic growth rate	Theoretical maximum of 10, precise value fitted from model.
B	Daily bite rate of vectors	The lower bound if 1/gonotrophic cycle, precise value fitted from model.
b	Daily rate at which vectors bite humans	b=B*HBI
γ	Daily probability of vector becoming infected after infectious bite	Fitted
c	Time delay for vector from infection to infectious stage	Sporogonic cycle, Calculated using Detinova formula 111/(T°C-18)
K_t	Environmental carrying capacity	$K_t = Pmm * akt$

Model implementation, simulation and testing

The model was implemented on a Microsoft Excel sheet using a set of difference equations with one day step. Each of the variables representing the human and mosquito subpopulations was followed in a separate column. In addition, at each stage, the model calculated the daily changes of these variables. An offset function was used for processes with delay, such as mosquitoes becoming infectious at the end of the sporogonic cycle. The model was driven by temperature, which defines the sporogonic cycle, and by rainfall. Both meteorological values were used to calculate the carrying capacity ($\mathbf{k_t}$)

The model's *goodness of fit* was determined using the residual sum of squares (SS) of the difference between the predicted and the observed values of all months. The value of each parameter was determined successively by minimizing SS (Table 2). This was continued for all parameters, until no further improvements in fit were possible, which was the common minimum for all parameters. The Microsoft Excel "Solver Add-In" function, which uses the Generalized Reduced Gradient (GRG2) method, was used for this process.

Table 2: Model parameter values and bounds

Parameters	Cissé[bounds]	Goni[bounds]	Nouna[bounds]
α	0.000126	0.000126	0.000126
β_1	0.000096	0.000096	0.000096
β_2	0.000041	0.000041	0.000041
q	0.12 [0.10-0.17]	0.12 [0.10-0.17]	0.12 [0.10-0.17]
v	10 days [9-15]	10 days [9-15]	10 days [9-15]

r	2	2	2
m	0.15[0.06-0.20]	0.15 [0.07-0.22]	0.14[0.05-0.22]
b	0.56[0.5-0.6]	0.56[0.5-0.6]	0.56[0.5-0.6]
γ	0.79	0.79	0.79
c	10.6 days [9-14]	13.3 days [9-14]	9.9 days [9-14]

The model predicted mosquito abundance and malaria incidence for each month, site for year 2004. Output values were normalized versus the expected, by multiplying each predicted monthly value by a ratio which was obtained by dividing the observed highest value by the predicted value month. The variance for the normalized prediction and observed values were calculated to assess the fit of the model for each site. Small variance suggests good representation of the field data by the model. The fit also was presented graphically, by plotting the monthly predicted and observed values.

Results

During follow up, out of the 676 children, 20 (3.0%) left the cohort, either because of death (11) or migration out of the study sites (9). Children were not always present at each visit; therefore, the overall person-years (PY) observed were 594.9.

Plasmodium falciparum malaria infection incidence

Out of 1274 fever episodes, 635 were positive for *Pf* malaria infection, giving an infection incidence of 1.1 episodes per PY. The lowest incidence was observed in Nouna (0.8 per PY). In Cissé and Goni, the incidences were 1.2 and 1.3, respectively, but not significantly different. There was strong seasonal variation in the incidence, with the peak August and September (Figure 2)

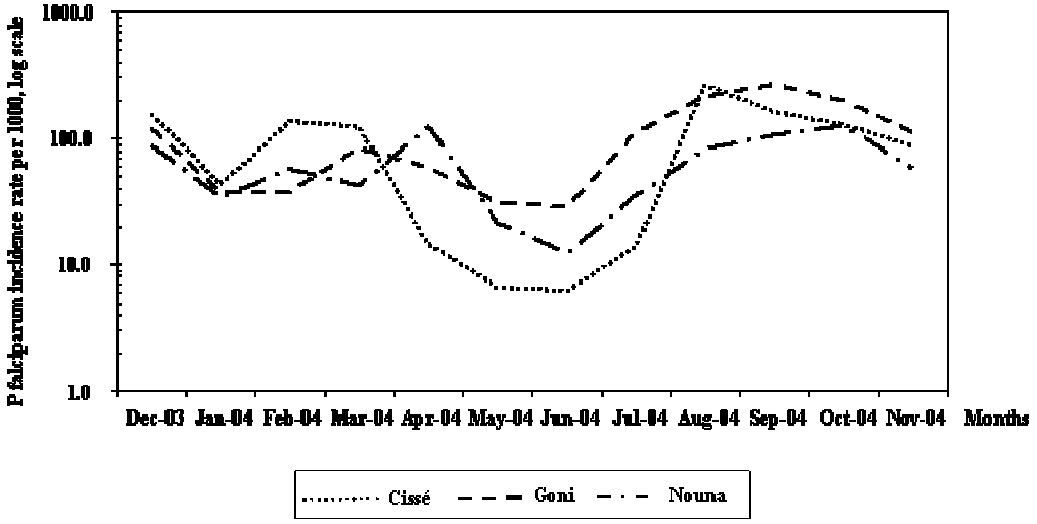

Figure 2 ***Plasmodium falciparum*** **malaria infection incidence rates, per month and site**

Entomological patterns

Using the LT and HLC method combined, with all species included across all sites, 16657 mosquitoes were caught. The largest proportion of captured mosquitoes was *Culex* (72.19%), followed by *An. gambiae* (15.57%), *Aedes* (6.3%), *Mansonia* (4.6%), *An. funestus* (1.5%) and *An. nili* (0.1%). The highest number of *An. Gambiae was* caught in Goni (n=1431), followed by Cisse (n=598) and Nouna (n=565).

Meteorological conditions

All sites presented a similar pattern of meteorological conditions. The rainfall was concentrated in the months from May to October. The total amount of rainfall was higher in Nouna than in Cissé or Goni .The relative humidity pattern followed that of rainfall. The mean temperature was more or less similar at all sites. The average mean temperature for the whole period was lower in Goni, however, with high variation versus Cissé and Nouna. Detail description of the meteorological condition is give elsewhere [20]

Model simulation

Simulation of daily *Anopheles gambiae* abundance

At all three sites, rainfall was followed by an increase in the mosquito population two weeks later (Figure 3).

In Cissé, mosquitoes were few (fewer than ten per day) over the first 120 days of the year, corresponding to January through April. The first peak in mosquito numbers was observed on the 122nd day of the year, followed by a second peak, one month later. These peaks all were observed after a peak in rainfall. Two other peaks in mosquito abundance were observed after the second peak. These increases corresponded to July and August, months with high rainfall. From August on, the vector population decreased significantly toward the end of year, after the end of the rainy season.

In Goni, the simulation produced several peaks in the vector population, following each peak in rainfall. As in Cissé, these peaks were clustered within a period from the 121st to 301st days of the year. This period corresponds with May through October. In contrast to Cissé, although there was some daily variation, the vector population remained high over this period, probably because of the higher amount of rainfall. After the end of the rainy season, we observed a drop in the mosquito population.

The Nouna site had about the same pattern of mosquito abundance and distribution as Goni, even though rainfall was more abundant. The mosquito population increased shortly after the onset of the rainy season. It remained high (about 100/ day), with some variation until the end of the rainy season, when levels decreased to less than ten mosquitoes daily. As at the two other sites, the highest peak in the mosquito population was observed about two weeks after the highest peak of rainfall in the August.

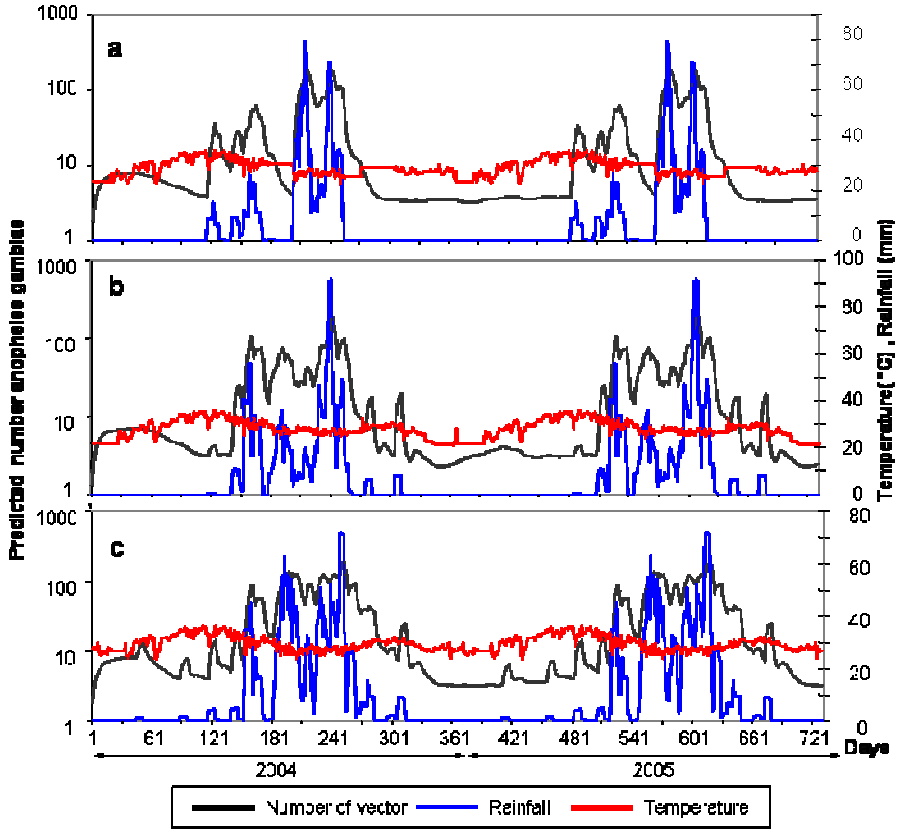

Figure 3: Mean temperature and rainfall-based predictions of *An. gambiae* population abundance for each site: a) Cissé, b) Goni and c) Nouna.[1]

Monthly prediction of *Anopheles gambiae* abundance compared to observed vector numbers

The model predicted a peak in vector numbers for all sites in September, matching the observations for Goni and Nouna (Figure 4). In Cissé, the peak in the number of caught mosquitoes was observed one month earlier, in August; this, therefore, did not match the prediction. Consistent across all sites, the model prediction matched with observed numbers from January through April, though the numbers were small. In June, in Cissé and Goni, there was a predicted increase in mosquito population which was not observed in the field. At all three sites, there was a significant decline (both predicted and observed) in the vector population in October, and both remained low in November and December.

[1] Simulated An. gambiae population abundance (black curve) is plotted against the daily temperature (red curve) and the preceding two weeks' cumulative rainfall (blue curve). The simulation was done daily for two years (2004 and 2005). The year 2004 was considered to be the training (warm-up) period of the model. As temperature and rainfall data for the year 2005 were not yet available, the conditions were assumed to be similar to 2004; therefore, temperature and rainfall were replicated.

Overall, the model predictions fit the observed data. The fit was better in Nouna, where we observed the least variance ($\Delta = \sum (O_i - P_i)^2 =$ 1696.5, SD=8.8); where O_i is the observed number in the vector population in the month, and P_i is the number predicted by the model. The variances for Goni and Cissé were 11630.4 and 35292.2, respectively.

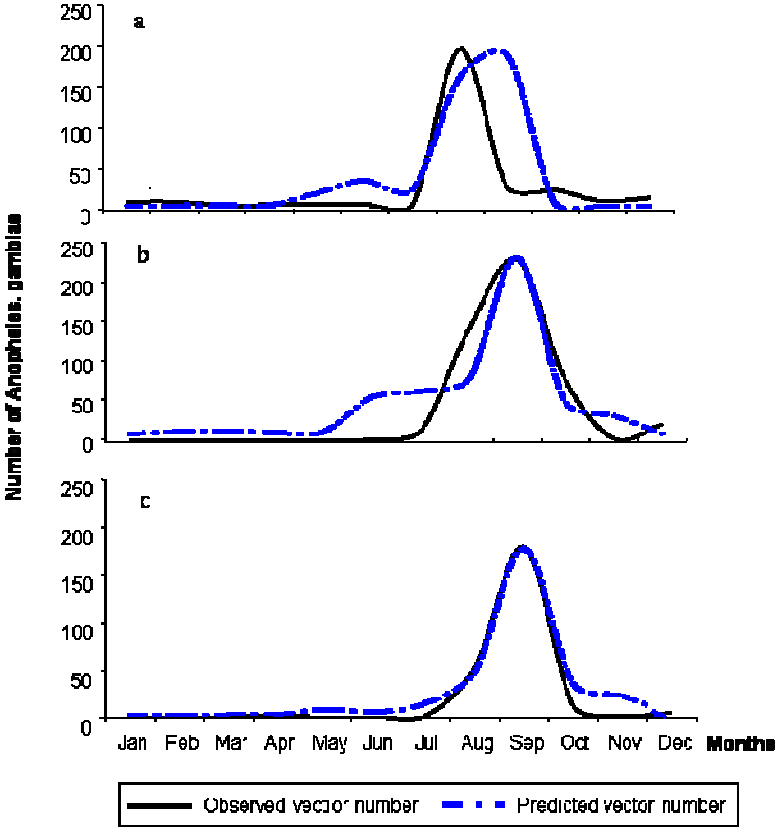

Figure 4: Predicted monthly *An Gambiae*, compared to observed vector numbers in Cissé (a), Goni (b) and Nouna (c). The monthly prediction (broken line) of *An. gambiae* is compared with those caught in the field (full line).

Monthly predicted *P falciparum* malaria infection episodes compared to observed

Incident cases of *Pf* malaria infection among children also were simulated by the model, per site and per month (Figure 5). For all sites, there was a seasonal pattern in *Pf* infection incidence. From December through June, the incidence decreased progressively, and then increased from July through September, after which another decrease was observed. Although the predicted and observed incidences were similar, there were some specific variations, expressed by the variation Δ. The model predictions match the observed episodes better in Goni, where the smallest variance was observed (Δ=626.8 SE=6.6), versus Nouna (Δ=733.7, SE=4.8) and Cissé (Δ=882.8, SD=6.7).

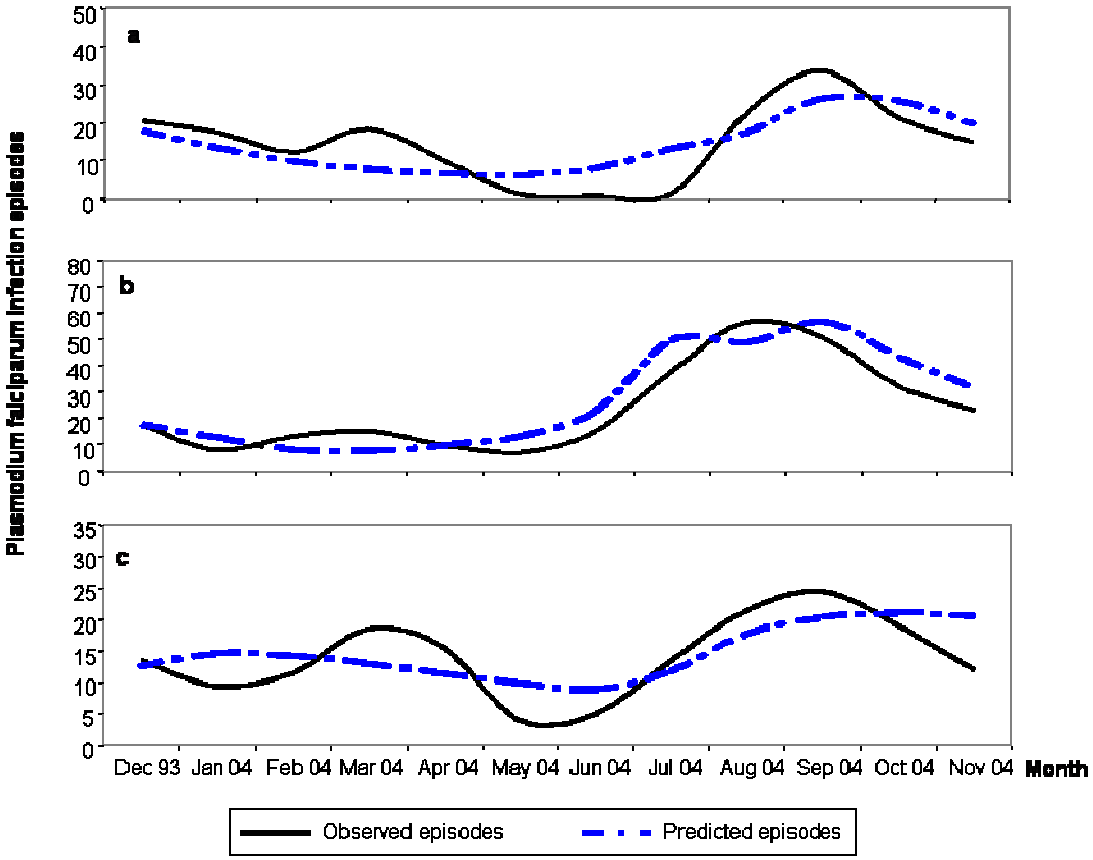

Figure 5: **Predicted monthly *Plasmodium falciparum* infection episodes versus observed episodes in Cissé (a), Goni (b) and Nouna (c)**

Discussion

A dynamic model to predict malaria transmission among children under age five was developed. The model is composed of five difference equations that express changes in infectious status of the human and vector populations given temperature and rainfall conditions. The model simulated the vector population abundance and the human *P falciparum* malaria infection incidence for each of three ecological settings over one year. Most of the model parameters were calculated based on field data, and fitted. The model was a good representation of *P falciparum* malaria infection in the region. The predicted mosquito populations and *P falciparum* malaria infection incidences were close to observed values.

Simulation of mosquito dynamics

Rainfall and temperature drive the vector population abundance. The dynamic model represented this adequately at all sites. Peak vector numbers observed about two weeks after a peak in rainfall is characteristic of the vector–rainfall relationship. Indeed, in ideal temperatures (28°C) and conditions, the development of *An. gambiae* from the egg to adult stage takes about 14 days [25, 29]. The presence of water pools generated by rainwater allows the mosquitoes to lay their eggs, which then develop into adult

mosquitoes if the water pools are sustained for at least 14 days. Some potential breeding sites could be expected in the area surrounding wells throughout the year. This is because of the constant spillage of water when people are fetching it. Sometimes, an intentional pool is created for purposes of watering cattle. However, these pools are not common and only produce a few the mosquitoes. Because of the dry conditions of the area, the most important source of breeding sites remains rainfall water, and this explains the high abundance of mosquitoes during the rainy season. Rainfall was the main driver of vector abundance. As expected, at all sites the model detected few vectors (less than ten) during the dry season; vectors persisted, despite the total absence of rainfall during this season, probably because of breeding sites created around wells.

Monthly predictions of the number of vectors fit the numbers caught in the field, and, both predicted and observed numbers followed a similar pattern at all sites. This suggests the model is a good representation of mosquito population dynamics. Some difference in the timing of peak abundance was observed in Cissé; where there was a deviation of one month between the predicted (September) and observed (August) peak. This may have been because of the soil texture in Cissé, which probably was not able to hold water on the surface long enough to allow the vector development. However, this was not captured by the current model. Consistent across all sites, the model predicted vectors in May and June, though no vectors were observed in the field. This could be explained by the model being sensitive to any amount of rainfall; whereas, in the field, the quantity of rainfall in May and June was not enough to keep vector breeding sites.

Although the model produced a fair representation of the mosquito population, it could be improved by also simulating the immature stage (eggs, larvae, pupae) of the vector, which is strictly dependant on surface water availability. Mosquitoes need water to produce and the ovi-position rate is assumed to be proportional to mosquito numbers and the daily rainfall filling local water pools [16]. Further, direct correlation of rainfall amount with mosquito abundance could result in some estimation bias. This is because the availability and duration of surface water also is dependant upon the evaporation index, soil texture and moisture index. High evaporation will cause quick-drying out of pools, whereas a lower consistency of soil texture and dry soil will lead to faster infiltration.

Simulation of *Plasmodium falciparum* malaria infection cases

Although some monthly differences were observed, probably due to the small number of cases, the general seasonal pattern was represented well by the model. However, the model is not sensitive to the sporogonic cycle. This implies that a small variation in ambient temperature would not result in major changes in incidence, and that time from human infection to gametocyte development is not a key in determining incidence rates.

The daily vector bite rate was found to be 0.56 per day. This would represent a gonotrophic cycle of 1.5 days, if every bite achieves a full blood meal. However, this is not always the case, as mosquitoes often return for second bites, if interrupted during their meal. Thus, the gonotrophic cycle may be longer than predicted by this model. The

model is insensitive to precise values of ***b***, (human bites per day) and this reduces the validity of the model as an estimator of gonotrophic cycle length. In addition, the model was developed assuming all vectors are *anthropophillic,* which is not necessarily the case. In fact, we expect this parameter to vary from one season to another [30].

The incidence of *P falciparum* malaria is dependent on two key parameters, which are the daily mortality rate of the vector and the parasite clearance rate in humans. These parameters both can be influenced by public health interventions. The daily mortality rate of the vector can be increased by vector control methods, such as indoor residual spraying, and vector numbers can be reduced by removing breeding sites. Effective treatment of patients will increase the malaria clearance rate in human (q), by protecting not only sick individuals, but also the surrounding population. The parasitological clearance rate (12%) was slightly slower than can be deduced from Müller and others. [31], who witnessed 27% seven-day parasitological failure with choroquine treatment. This would reflect 17% daily clearance. This discrepancy probably is a result of Müller and colleagues [31] having measured the asexual form clearance, while our focus was on the sexual form.

The model is driven by parasitological data for children under five, while the entire population contributes to the transmission. To account for this effect, we would need to survey the general population. This would require checking large numbers of asymptomatic individuals for subclinical infections. This raised technical and ethical issues. Nevertheless, it was assumed the parasite prevalence among children under five was not unlike that of the general population, even though clinical symptoms will not be present in many older individuals.

The model can be a useful tool for malaria control strategies especially in a low transmission context. It has the ability of quantifying the context specific risk of malaria, a precondition for cost-effective interventions. Although, the model was developed based on data collected in a specific context it can be used in a different setting. In that case the parameters would have to be measured locally and fitted without the need to change the model formulation. The fitting of the model was based on field data to make sure that mathematic formulas are plausible and describe the biological process of the transmission of the disease. To be used to predict malaria incidences in other settings the critical inputs will be rainfall and temperature data, which nowadays can be obtained for satellite sources. Other parameters maybe fitted of obtained from literatures

Other strength of the model lies in its simplicity and its respect for the biological process of malaria transmission on the ground. However, to be cost-effective, the model major drivers which are rainfall and temperature could be derived from remote sensing data as ground based measurements are expensive to implement at local scale.

Conclusion

The model shows potential for local-scale seasonal prediction of *P falciparum* malaria infection rates and distribution. Thus, it could be used to understand malaria transmission

dynamics, using meteorological parameters as a driving force, to help local district health bodies to identify the risk period for more focused intervention. However, we do not pretend to have captured 100% of the transmission dynamics. Further improvement to the model can be made.

References

1. Ross R: Studies on Malaria. John Murray, London 1928.

2. Utzinger J, Tozan Y, Singer BH: **Efficacy and cost-effectiveness of environmental management for malaria control.** *Trop Med Int Health* 2001, **6**: 677–687.

3. Macdonald G: Appendix I. Mathematical statement. In: The Epidemiology and Control of Malaria, Oxford University Press; London. pp 201, 1957

4. Dietz K, Molineaux L, Thomas A: **Malaria model tested in the savannah**. *Bull World Health Organ* 1974, **50**:347-357.

5. Molineaux L, Gramiccia G: The Garki Project. World Health Organization, p 311, Geneva 1980.

6. McKenzie FE, Samba EM: **The role of mathematical modeling in evidence-based malaria control**. *Am J Trop Med Hyg* 2004, **71**: 94-6.

7. Halloran ME, Struchiner CJ, Spielman A: **Modellingmalaria vaccines. II: Population effects of stage-specific malaria vaccines dependent on natural boosting**. *Math Biosci* 1989, **94**: 115–149.

8. Randolph SE, Rogers DJ: **Satellite data and disease transmission by vectors: the creation of maps for risk prediction**. *Bull Soc Pathol Exot* 2000, **93**:207.

9. Kleinschmidt I, Sharp BL, Clarke GP, Curtis B, Fraser C: **Use of generalized linear mixed models in the spatial analysis of small-area malaria incidence rates in Kwazulu Natal, South Africa**. *Am J Epidemiol* 2001, **153**: 1213-21

10. Hay SI, Omumbo JA, Craig MH and Snow RW: **Earth observation, Geographic Information Systems and *Plasmodium falciparum* Malaria in Sub-Saharan Africa, Remote Sensing and Geographical Information System in epidemiology**, Volume 47 Oxford, UK, pp 173-215, 2000.

11. Rogers DJ, Randolph SE, Snow RW, Hay SI: **Satellite imagery in the study and forecast of malaria.** *Nature* 2002, **415**: 710-5.

12. Craig MH, Snow RW, le Sueur D: **A climate-based distribution model of malaria transmission in sub-Saharan Africa.** *Parasitol Today* 1999, **15**: 105-11.

13. MARA/ARMA: **Towards an Atlas of Malaria Risk in Africa. First Technical Reports of the MARA/ARMA collaboration**, Durban, 1998

14. Martens WJ, Niessen LW, Rotmans J, Jetten TH, McMichael AJ: **Potential impact of global climate change on malaria risk**. *Environ Health Perspect* 1995, **103**: 458-64.

15. Lindsay SW, Martens WJ: **Malaria in the African highlands: past, present and future**. *Bull World Health Organ* 1998, **76**: 33-45.

16. Hoshen MB, Morse AP: **A weather-driven model of malaria transmission**. *Malaria J* 2004, **3**: 32.

17. Garnham PCC: **Malaria in Kisumu, Kenya colony**. *Journal of Tropical Medicine and Hygiene* 1929, 32: 207-216

18. Yé Y, Sanou A, Gbangou A, Kouyaté B: INDEPTH. Demography and Health in Developing Countries. Volume 1. Population, Health and Survival at INDEPTH Sites. Chapter 19 Nouna DSS. IDRC Canada.2002

19. Yé Y, Kyobutungi C, Louis RV, Sauerborn R: **Micro-epidemiology of *Plasmodium falciparum* malaria: Is there any difference in transmission risk between neighbouring villages?** *Malaria J***,** 2007 in press

20. Yé Y, Louis V, Simoboro S, Sauerborn R: Effect of meteorological factors on clinical malaria risk among children, using village-based meteorological stations and community-based parasitological survey. BMC Public Health 2007, in press

21. Cano J, Berzosa PJ, Roche J, Rubio JM, Moyano E, Guerra-Neira A, Brochero H, Mico M, Edu M, Benito A: **Malaria vectors in the Bioko Island (Equatorial Guinea): estimation of vector dynamics and transmission intensities**. *J Med Entomol* 2004, **41**: 158-61.

22. Detinova TS: **Méthodes à appliquer pour classer par groupes d'âge les diptères présentant une importance médicale**. *Ser Monogr WHO N°27*, Geneva, 1993

23. Gilles HM, Warrell DA: Bruce-Chwatt's Essential Malariology, Third edition. Edward Arnold, London, 1993

24. Takken W, Klowden MJ, Chambers GM: **Effect of body size on host seeking and blood meal utilization in *Anopheles gambiae* sensu stricto (Diptera: Culicidae): the disadvantage of being small.** *J Med Entomol* 1998, **35**: 639-645.

25. Depinay JM, Mbogo CM, Killeen G, Knol B, Beier J, Carlson J, Dushoff J, Billingsley P, Mwambi H, Githure J, Toure AM, McKenzie FE: **A simulation model of African Anopheles ecology and population dynamics for the analysis of malaria transmission**. *Malar J* 2004, **3**: 29.

26. Rogers DJ: In Youdeowei A and Service MW Pest and vector management in the tropics with particular reference to insects, ticks, mites and snails. pp 139-159, London: Longman, 1983.

27. Mckenzie FE, Wong RC, Bossert WH: **Discrete-event simulation models of Plasmodium falciparum malaria**. *Simulation*, 1998 71: 250-61.

28. Yé Y, Sauerborn R, Simoboro S, Hoshen Moshe: **Using modelling to assess malaria infection risk during the dry season on a local scale in an endemic area of rural Burkina Faso.** *Ann.Trop.Med Parasitol* 2007, *in press, July issue*

29. Jepson WF, Moutia A, Courtois C : **The malaria problem in Mauritius: The binomics of Mauritian anophelines**. *Bull Entomol Res* 1947, **38**:177-208.

30. Awolola TS, Okwa, Hunt RH, Ogunrinade AF, Coetzee M: **Dynamics of the malaria vector populations in coastal Lagos, south-western Nigeria.** *Ann.Trop.Med Parasitol* 2002, 96: 75-82.

31. Müller O, Traoré C, Becher H, Kouyate B: **Malaria morbidity, treatment-seeking behaviour, and mortality in a cohort of young children in rural Burkina Faso**. *Trop Med Int Health* 2003, 8: 290–296.

32. Detinova TS: **Age-grouping methods in Diptera of medical importance with special reference to some vectors of malaria**. *Monogr Ser WHO N° 47*, Geneva; 1962.

Appendix: Model description

The dynamic concept in contrast to the static concept, tries to capture the transmission and biological processes of the disease. The model was based on the assumption that the human population is divided into three categories: Susceptible (S), Malaria- infected (I) and infectious (G) and mosquito population is classified into two compartments: non-infections (U) and infectious.

$$\delta S = \alpha(S+I+G) + q(I+G) - \left(1 - \left(\frac{S+I+G-1}{S+I+G}\right)^{bF}\right)S - \beta_1 S \qquad \textbf{(1)}$$

$$\delta I = \left(1 - \left(\frac{S+I+G-1}{S+I+G}\right)^{bF}\right)S - (1-(\beta_1+\beta_2+q))^{v}\left[\left(1 - \left(\frac{S+I+G-1}{S+I+G}\right)^{bF}\right)S\right]_{t-v} - (\beta_1+\beta_2+q)I \qquad \textbf{(2)}$$

$$\delta G = (1-(\beta_1+\beta_2+q))^{v}\left[\left(1 - \left(\frac{S+I+G-1}{S+I+G}\right)^{bF}\right)S\right]_{t-v} - (\beta_1+\beta_2+q)G \qquad \textbf{(3)}$$

$$\delta U = \frac{r(U+F)}{\left[1+\frac{(U+F)}{K_t}\right]} - \left[bU\frac{G}{S+I+G}\right]_t \gamma - mU \qquad \textbf{(4)}$$

$$\delta F = (1-m)^{c}\left[bU\frac{G}{S+I+G}\right]_{t-c}\gamma - mF \qquad \textbf{(5)}$$

Equations 1-3 describe the change in the human population while equations 4-5 describe change in vector population. Each term is explained in detail below

Change in uninfected human population

$$\delta S = \alpha(S+I+G) + q(I+G) - \left(1 - \left(\frac{S+I+G-1}{S+I+G}\right)^{bF}\right)S - \beta_1 S \qquad \textbf{(1)}$$

Equation 1 describes the changes in the uninfected human population and includes four terms:

- The first term is the natural growth rate which is expressed by $\alpha(S+I+G)$, assuming people are born healthy and irrespective of the health of the mother. As the model is simulated daily, this is expected to be negligible.
- The second term is the malaria clearance expressed by $q(I+G)$. We assume that people clear the infection at a fixed rate from all stages of the disease. We also assume that there is no immunity and no superinfection (additional infection starts after a new hepatic stage), contrary to *Dietz et al* (1974)
- The third term is the human infection expressed by $\left(1 - \left(\frac{S+I+G-1}{S+I+G}\right)^{bF}\right)S$. It expresses the daily new infection within the human population. The expression

$\frac{S+I+G-1}{S+I+G} = 1 - \frac{1}{S+I+G}$ is the probability of a single person not getting a bite from a specific mosquito; *b*F is the number of infectious mosquito biting in a day, given a daily biting rate per mosquito of *b,* $\left(\frac{S+I+G-1}{S+I+G}\right)^{bF}$ is the probability of a specific person not getting bitten by any of the infectious mosquitoes. $1-\left(\frac{S+I+G-1}{S+I+G}\right)^{bF}$ is the probability of a specific person getting bitten by one or more of infectious mosquitoes. Multiplying by S gives the number of uninfected peoples being bitten by at least one infectious mosquito in a day.

- The fourth term is ***/3₁*** the death rate in the population from all causes except malaria, assuming there is not link with malaria. Then ***/3₁S*** is the number of death within the uninfected population.

In addition the following assumptions were made

1 A mosquito bites only once in a gonotrophic cycle.
2 Mosquitoes bite randomly. No specific attraction to any sub population.
3 The stage of infection does not influence the mosquitoes biting habits.
4 An infectious bite necessarily causes *Plasmodium falciparum* infection.

Change in infected human population

$$\delta I = \left(1-\left(\frac{S+I+G-1}{S+I+G}\right)^{bF}\right)S - (1-(\beta_1+\beta_2+q))^{v}\left[\left(1-\left(\frac{S+I+G-1}{S+I+G}\right)^{bF}\right)S\right]_{t-v} - (\beta_1+\beta_2+q)I \quad \textbf{(2)}$$

Equation 2 describes the changes in the infected (but not infectious) human population and includes three terms:

- The first term is $\left(1-\left(\frac{S+I+G-1}{S+I+G}\right)^{bF}\right)S$ and as described above is the number of uninfected people being bitten by at least one infectious mosquito in a day.
- The second term $\left[\left(1-\left(\frac{S+I+G-1}{S+I+G}\right)^{bF}\right)S\right]_{t-v}$ represents people that became infected ***v*** days ago. They have now mature gametocytes and are infectious. However not all of those people are still available. They may have either died of malaria or other disease or they may have cleared their infection. For each day the probability of leaving the group early will be ***/3₁ +/3₂ +q***. The probability of remaining in the group for a day is $1-(\beta_1+\beta_2+q)$ **.** The probability of completing the whole process of ***v*** days is $(1-(\beta_1+\beta_2+q))^{v}$
- The third term $-(\beta_1+\beta_2+q)I$ represents the number of people that leave the infected stage by death or clearance.

In addition, the following assumptions were made:

1. ***/3₂*** is constant and does not change according to the stage of the infection. We know the mortality could change per stage. We may leave it out of this equation for biological reasons.
2. ***q*** is not specific to the stage of the infection. We have two types of ***q***.

clearance because of treatment and clearance because of immune system (natural clearance). We could also decide there is no natural clearance. We also know that drugs are stage specific (liver stage, blood stage).

Change in infectious human population

$$\delta G = (1-(\beta_1+\beta_2+q))^{v}\left[\left(1-\left(\frac{S+I+G-1}{S+I+G}\right)^{bF}\right)S\right]_{t-v} - (\beta_1+\beta_2+q)G \qquad \textbf{(3)}$$

Equation 3 describes the changes in the infectious human population and includes two terms.

- The first term $(1-(\beta_1+\beta_2+q))^{v}\left[\left(1-\left(\frac{S+I+G-1}{S+I+G}\right)^{bF}\right)S\right]_{t-v}$ is described above.
- The second term, $-(\beta_1+\beta_2+q)G$ represents the number of people that leave the infectious stage by death or clearance

Change in the size of uninfected vector population

$$\delta U = \frac{r(U+F)}{\left[1+\frac{(U+F)}{K_t}\right]} - \left[bU\frac{G}{S+I+G}\right]_t \gamma - mU \qquad \textbf{(4)}$$

Equation 4 describes the changes in the uninfected vector population and includes three terms.

- The first term $\frac{r(U+F)}{\left[1+\frac{(U+F)}{K_t}\right]}$ is the maturation of the larval stage. This term describes the number of larvae surviving to become mature mosquitoes. The numerator is the number of larvae expected to survive to maturity under ideal conditions. *U+F* is the total number of mosquitoes, assuming infectious status does not influence the fertility. ***r*** is the per mosquitoes fertility (number of eggs oviposited per day multiplied by the probability of each to develop into a mature mosquito under ideal condition). The denominator reflects the decrease in survival because of non-ideal conditions. The *U+F* expresses the density dependent limitation on larvae survival. The precise characteristic of this dependence is determined by the carrying capacity K_t. In principle, K_t varies with temperature, rainfall and humidity and should be measured from the field. Thus the number of larvae increases with the number of mosquitoes but is limited by carrying capacity. The number of the larvae surviving is dependent on the surface water available. As at this stage of research a full evapo-transpiration model is not available, K_t is therefore assumed to be proportional to the previous weekly aggregated rainfall. ***K_t =Pmm*akt.*** The value of ***akt*** is to be determined empirically.
- The second term, $bU\frac{G}{S+I+G}$ represents the new infections of mosquito at time ***t.*** *b*U is the number of uninfected mosquitoes biting in a day. The fraction is the

probability of a single mosquito biting at random an infectious human out of the total human population. We multiply this by **γ** to reflect the probability of becoming infected.

- The third term, ***mU,*** is the mortality of uninfected mosquitoes or the number of uninfected mosquitoes dying per day. *m* was calculated from the *k-value* (log generation mortality). In the study site setting, due to the constantly warm temperature, the gonotrophic cycle varies between 2 and 3 days. The survival of mosquitoes depends on the gonotrophic cycle and due to the stability of the cycle *m* was treated as constant. The precise value of *m* was empirically determined by fitting the model.

In addition the following assumptions were made:

1 Mosquitoes bite randomly and independent of their infectious status
2 Survival is independent of the infectious status

Change in the size of the infectious vector population

$$\delta F = (1-m)^c \left[bU \frac{G}{S+I+G} \right]_{t-c} \gamma - mF \qquad \textbf{(5)}$$

Equation 5 describes the changes in the infected vector population and includes two terms:

- The first term, $(1-m)^c \left[bU \frac{G}{S+I+G} \right]_{t-c} \gamma$ is the number of mosquitoes infected *c* days ago, reduced by the survival. *c* is the sporogonic cycle given by Detinova [32] as 111/(T°-18).
- The second term $-mF$ is the number of infectious mosquitoes dying in a day.

In addition the following assumptions were made:

1 Infectious mosquitoes never clear their infectious status.
2 Mosquitoes are either infected or infectious